Adaptive MMSE turbo equalization with high-order modulations and spatial diversity applied to underwater acoustic communications

Christophe Laot, Raphaël Le Bidan

Adaptive MMSE turbo equalization with high-order modulations and spatial diversity applied to underwater acoustic communications

Christophe Laot and Raphaël Le Bidan
Institut TELECOM ; TELECOM Bretagne ; LabSTICC CNRS UMR 3192,
Université européenne de Bretagne,
Technopole Brest-Iroise - CS 83818 - 29238 Brest Cedex 3, France
Email: christophe.laot@telecom-bretagne.eu, raphael.lebidan@telecom-bretagne.eu

***Abstract*— This paper presents some results on adaptive minimum mean-square error (MMSE) turbo equalization obtained from underwater experiments in the Atlantic ocean. The performance gain is evaluated as a function of the number of hydrophones at the receiver side. Single-carrier transmission with high-order modulations is considered, at a coded bit rate as high as 24 kb/s on the underwater acoustic channel. The all-digital receiver performs timing recovery, equalization, interleaving and channel decoding.**

I. Introduction

This paper presents a high data rate acoustic link between two boats in motion. The proposed receiver is based on the TRIDENT receiver [1], developed by GESMA (Groupe d'Etudes Sous-Marines de l'Atlantique, Brest, France), in collaboration with Telecom Bretagne and SERCEL. This receiver was designed for text, images and speech data transmission in a shallow water environment. Initially based on QPSK, the TRIDENT receiver has been extended in this paper to high-order modulations (8-PSK, 16-QAM and 32-QAM). This results in the transmission of coded bit rates as high as 24 kb/s over distances greater than 1 km.

To maximize the spectral efficiency of the link, a single-carrier modulation is used. Data transmission is organized into long bursts. In contrast to OFDM systems, this scheme avoids the spectral efficiency loss due to the insertion of a guard interval or a cyclic prefix. The proposed receiver must be able to deal with time- and frequency-selective channels. Therefore we use efficient synchronization schemes and an adaptive multiple-input equalizer. In addition, channel coding is used to increase the robustness of the transmission.

Minimum mean square error (MMSE) turbo equalization [2]–[4] has proven to be effective for removing intersymbol interference. The equalizer and the channel decoder exchange soft information in an iterative process. This allows the equalizer to benefit from the channel decoder gain, and *vice versa*. MMSE turbo equalization has already been considered for underwater acoustic communications [5]–[9].

This work was supported in part by GESMA/DGA, France.

In this paper, we evaluate the performance improvement provided by the adaptive MMSE turbo equalizer as a function of the number of hydrophones at the receiver side. It is shown that, as expected, the performance improves when the number of hydrophones increases. As the spatio-temporal equalizer combines the signals received from the different hydrophones, the signal-to-noise ratio (SNR) at the output of the equalizer increases, thereby providing a performance gain possibly greater than $10\log_{10}(N_R)$ dB, where N_R is the number of hydrophones. Since the channel diversity combining realized by the multiple-input equalizer drastically reduces the intersymbol interference (ISI), the performance improvement provided by the turbo equalizer is usually small. On the other hand, if only one hydrophone is used, a linear equalizer without *a priori* information usually results in poor performance. In this case, the performance gain provided by the turbo equalizer can be significant. This observation is particularly interesting in an industrial context since a reduction of the number of hydrophones may translate into significant costs savings and allow a diminution of the equipments size.

Sections II-III are quite similar to those in the previous paper [9]. The main contribution of this paper appears in section IV, where new experimental results are given on the performance of turbo equalization using high-order modulations.

II. Transmission model

The transmission scheme is depicted in Figure 1. A rate-R_c convolutional code is fed by binary data α_n. An interleaver Π shuffles the coded bits $c_{n,i}$. Each set of $m = \log_2(M)$ interleaved coded bits $c_{k,i}$ is mapped onto an M-ary complex symbol d_k taken from an M-PSK or M-QAM signal set, using Gray or quasi-Gray labeling. Data transmission is organized into bursts. Each burst is made of an initial preamble dedicated to frame detection and synchronization, followed by several fixed-size data blocks separated by pilot sequences. A transducer transmits the modulated signal on the time- and frequency-selective underwater channel. The receiver is equipped with a chain of N_R hydrophones spaced 25cm apart.

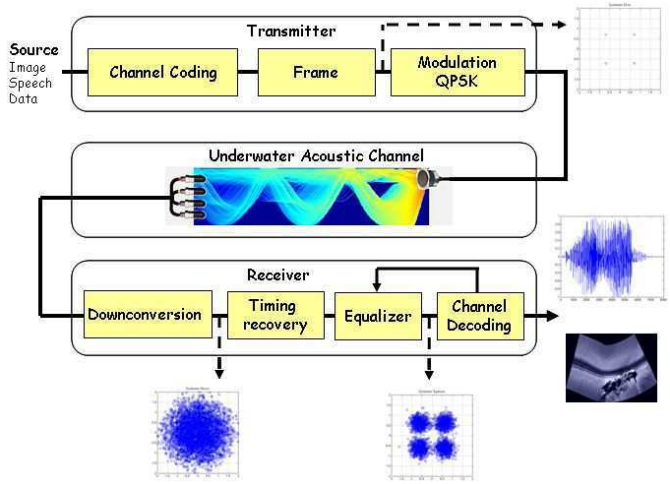

Fig. 1. Single-carrier transmission scheme overview

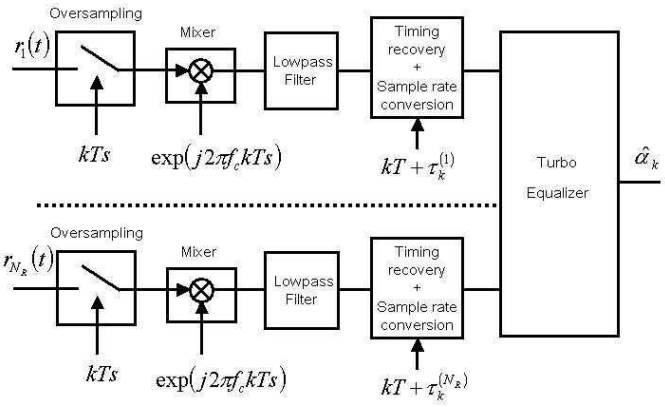

Fig. 2. Structure of the all-digital receiver

An all-digital single-carrier receiver is used, relying on a multiple-input adaptive MMSE turbo equalization scheme.

Let $s(t)$ be the transmitted waveform:

$$s(t) = \Re e\{ \sum_{n=-\infty}^{+\infty} d_k g(t - kT) e^{j(2\pi f_c t + \psi)} \} \qquad (1)$$

where f_c is the carrier frequency, ψ is the carrier phase uncertainty, $1/T$ is the symbol rate with T the symbol duration, $\{d_k\}$ are the transmitted symbols with variance σ_d^2, and $g(t)$ is a square-root raised-cosine filter with roll-off factor 0.25.

Since the signal is centered on a relatively low carrier frequency ($f_c = 17.5$kHz in our experiments - see Section IV), an all-digital receiver is feasible [10]. Oversampling is performed at the rate $1/T_s$ where T_s is chosen so as to satisfy the sampling theorem. In this paper, we have chosen $T = 20T_s$. The down-conversion is performed digitally, and a timing synchronization scheme based on a sample rate converter is used to determine the optimum sampling time. The resulting all-digital receiver is depicted in Figure 2.

In wide-band transmission, as is the case in underwater acoustic communications [11], [12], the Doppler effect introduces a scaling of the symbol period which must be taken into account in the design of the timing recovery scheme [13], [14]. The optimum sample time not only depends on the propagation delay at hydrophone $j; j = 1, \ldots, N_R$ but also on a common Doppler shift depending on the relative speed of the boats and the propagation wave velocity [13]–[16]. Because the receiver is all-digital, the optimum sampling time $kT + \tau_k^{(j)}$ is not necessarily a multiple of T_s. A sample rate conversion based on interpolation, filtering and decimation is then required [10].

The optimum sampling time is unknown and must be estimated. Initial compensation of the common Doppler shift is performed by using the short preamble inserted at the beginning of the transmission to estimate the relative velocity [17]. Note that this preamble is also used to perform frame detection and synchronization. Then, a non-data-aided (NDA) timing recovery scheme is designed which takes into account the residual Doppler shift due to the moving platforms and the different channel delays at each antenna [18], [19].

After demodulation, sampling, Doppler compensation and timing recovery, the received signal can be modeled by the output of a single-input multiple-output (SIMO) discrete-time channel where each output $j; j = 1, ..., N_R$ is corrupted by an additive noise $w_k^{(j)}$ with variance $\sigma_{(j)}^2$. The signal $r_k^{(j)}$ received on antenna j at time kT can be written as:

$$r_k^{(j)} = \sum_{l=0}^{L^{(j)}} h_{k,l}^{(j)} d_{k-l} + w_k^{(j)} \qquad (2)$$

where $\{h_{k,l}^{(j)}\}$ are the $L^{(j)} + 1$ coefficients of the multi-path time-varying channel seen by antenna j at time kT.

III. Turbo-equalization principle

The adaptive turbo equalizer is depicted in Figure 2. Equalization and channel decoding exchange soft information in an iterative manner. Each iteration consists of a multiple-input equalizer, a soft-input soft-output (SISO) demapper, a deinterleaver Π^{-1}, a binary SISO channel decoder, an interleaver Π and a SISO mapper. The equalizer is fed in by the received signal samples $r_k^{(j)}$ and also by the estimated data $\bar{d}_k$ obtained from the previous iteration. The channel decoder delivers hard-decisions $\hat{\alpha}_n$ on the information bits for the current iteration. It also provides soft decisions on the coded bits, which are used in turn by the SISO mapper to compute the soft symbol estimates $\bar{d}_k$ to be used by the equalizer in the next iteration.

A. SISO mapping

The soft estimate $\bar{d}_k$ on the transmitted data symbols is computed from the log-likelihood ratios (LLRs) on the coded bits delivered by the SISO channel decoder. Specifically, the soft estimate $\bar{d}_k$ is defined as the mathematical expectation of symbol d_k, and is given by $\bar{d}_k = \sum_{s \in \mathcal{S}} s \times P_a(d_k = s)$, where $\mathcal{S}$ is the considered M-PSK or M-QAM signal set. The term $P_a(d_k = s)$ denotes the *a priori* probability that symbol d_k takes the particular value s in the signal set. It is related to the *a priori* probabilities on the encoded bits $c_{k,i}; i = 1, \ldots, m$ that are mapped onto symbol d_k. Assuming that the encoded

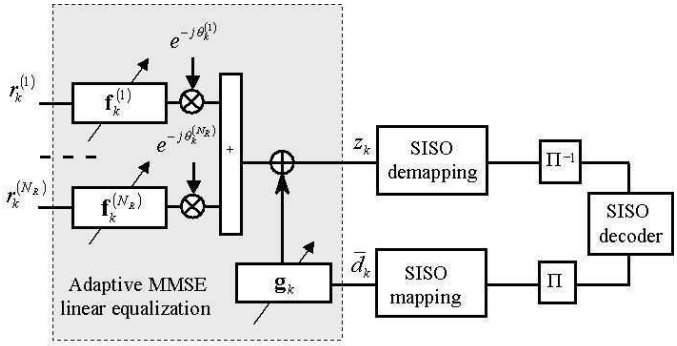

Fig. 3. Turbo-equalization scheme

bits are statistically independent (thanks to the interleaving), we obtain:

$$P_a(d_k = s) = \prod_{i=1}^{m} P_a(c_{k,i} = s_i) \tag{3}$$

where $s_i \in \{0,1\}$ is the value of the ith bit associated to symbol $s \in \mathcal{S}$ by the considered labeling rule. On the other hand, it can be shown that the *a priori* probability $P_a(c_{k,i})$ on a given coded bit $c_{k,i}$ and the corresponding *a priori* LLR $L_a(c_{k,i})$ coming from the channel decoder are linked by the following relation [20]:

$$P_a(c_{k,i} = j) = \frac{1}{2}\left(1 + (2j-1)\tanh\left(\frac{L_a(c_{k,i})}{2}\right)\right) \tag{4}$$

with $j \in \{0,1\}$.

B. Adaptive multiple-input equalizer structure

The adaptive equalizer is depicted in Figure 3. The multiple-input equalizer combines the outputs of the feedforward transversal filters fed by the signals received from the hydrophones. Second-order phase-lock loops (PLLs) are optimized jointly with the equalizer filters in order to compensate for the residual frequency offsets. When *a priori* information is available from the channel decoder at the previous iteration, a feedback filter fed in by the estimated symbols $\bar{d}_k$ is used to suppress the residual interference at the combiner output.

The filter coefficients of the equalizer are optimized so as to minimize the conditional mean square error $E\{|z_k - d_{k-\Delta}|^2|\{\bar{d}_k\}\}$ between the equalized symbol z_k at time k and the data symbol $d_{k-\Delta}$ transmitted at time $k-\Delta$.

An adaptive procedure is used to obtain the filter coefficients [2]. This adaptive algorithm is composed of two distinct phases: the training phase and the tracking phase. The training phase makes use of pilot sequences known to the receiver (data-aided (DA)) to initialize the equalizer coefficients. Next, during the tracking period, the coefficients are continuously updated in a decision-directed (DD) manner, based on the receiver decisions on the transmitted symbols.

The equalizer output z_k is given by:

$$z_k = \sum_{j=1}^{N_R} (\mathbf{f}_k^{(j)})^T \mathbf{r}_k^{(j)} e^{-j\theta_k^{(j)}} - \mathbf{g}_k^T \tilde{\mathbf{d}}_k \tag{5}$$

where $\tilde{\mathbf{d}}_k = \left(\bar{d}_{k+G}, \ldots, \bar{d}_{k-\Delta+1}, 0, \bar{d}_{k-\Delta-1}, \ldots, \bar{d}_{k-G}\right)^T$ is the vector of estimated symbols and $\mathbf{r}_k^{(j)} = \left(r_{k+F}^{(j)}, \ldots, r_{k-F}^{(j)}\right)^T$ is the vector of channel output samples received on hydrophone j, with respective lengths $2F+1$ and $2G+1$. Note that the coordinate relative to the soft estimate $\bar{d}_{k-\Delta}$ in $\tilde{\mathbf{d}}_k$ is set to zero in order not to cancel the signal of interest at time k. Vectors $\mathbf{f}_k^{(j)} = \left(f_{k+F}^{(j)}, \ldots, f_{k-F}^{(j)}\right)^T$ and $\mathbf{g}_k = (g_{k+G}, \ldots, g_{k-G})^T$ represent the coefficients of the feedforward filters and feedback filter, respectively. During the training phase, both vectors are updated on a symbol-by-symbol basis using a data-aided least-mean square (DA-LMS) gradient algorithm:

$$\begin{aligned} \mathbf{f}_{k+1}^{(j)} &= \mathbf{f}_k^{(j)} - \mu\,(z_k - d_{k-\Delta})\,(\mathbf{r}_k^{(j)} e^{-j\theta_k^{(j)}})^* \\ \mathbf{g}_{k+1} &= \mathbf{g}_k + \mu\,(z_k - d_{k-\Delta})\,\tilde{\mathbf{d}}_k^* \end{aligned} \tag{6}$$

where μ is a small, positive step-size that controls the convergence properties of the algorithm. During the tracking period, the DA-LMS is replaced by a decision-directed LMS (DD-LMS) which operates on the decisions $\hat{d}_{k-\Delta}$ computed from the equalizer output z_k.

We have therefore defined an adaptive MMSE equalizer whose coefficients are obtained from an LMS algorithm, thereby allowing tracking of the channel time variations.

C. SISO demapping

The role of this module is to convert the equalized data z_k into extrinsic LLRs on the interleaved coded bits, which will then be transmitted to the SISO (soft input soft output) channel decoder. Generally, we can always decompose the expression of z_k as the sum of two quantities:

$$z_k = g_0 d_{k-\Delta} + \nu_k \tag{7}$$

The term $g_0 d_{k-\Delta}$ represents the desired signal up to a constant factor g_0. The term ν_k accounts for both residual interference and noise at the output of the equalizer. Using a Gaussian approximation of the distribution of the residual ISI, it can be shown that ν_k follows a complex Gaussian distribution, with zero mean and total variance $\sigma_\nu^2 = \sigma_d^2 g_0(1-g_0)$, and where $0 \le g_0 < 1$ [20], [21]. The extrinsic LLR on the coded bits $(c_{k-\Delta,1}, \ldots, c_{k-\Delta,m})$ mapped onto data symbol $d_{k-\Delta}$ are then given by:

$$L_e(c_{k-\Delta,i}) = \ln \frac{\sum_{s\in\mathcal{S}:s_i=c_{k-\Delta,i}=1} \exp\left(-\frac{|z_k - g_0 s|^2}{\sigma_\nu^2}\right)}{\sum_{s\in\mathcal{S}:s_i=c_{k-\Delta,i}=0} \exp\left(-\frac{|z_k - g_0 s|^2}{\sigma_\nu^2}\right)} \tag{8}$$

In order to compute the extrinsic information $L_e(c_{k-\Delta,i})$, knowledge of the bias factor g_0 is required. From (7) and the expression of σ_ν^2, it can be easily shown that $g_0\sigma_d^2 = E\{|z_k|^2\}$. In practice, g_0 is estimated by computing the sample mean-square modulus of the equalized symbols $\{z_k\}$ on a block-by-block basis.

D. SISO channel decoder

The channel decoder is a SISO device which implements the Log-MAP algorithm [22]. The observations provided by the SISO demapper fed the channel decoder input which delivers soft-output decisions on coded data. This soft-output decisions fed in turn the SISO mapper which uses them to compute the soft estimates $\bar{d}_k$ on the transmitted symbols.

IV. Experimental results

Experimental sea trials were carried out on March 2010 in the site "bay of Brest", France, by DGA/GESMA. During these trials, data were transmitted between two boats in a shallow water environment. The water depth was about 10 to 30 meters. As depicted in Figure 4, the transmitter and the receiver were placed on the "Aventurière II" and "Idaco" ships, respectively. At the receiver side, the antenna array was a vertical chain of $N_R = 4$ hydrophones spaced 25cm apart.

In this paper, we focus on a particular sequence recorded to test the turbo-equalizer with high-order modulations. This sequence includes consecutive bursts of modulated symbols (8-PSK, 16-QAM and 32-QAM) separated by a guard interval of 5 seconds. Single-carrier transmissions with a carrier frequency of 17.5 kHz were used. The symbol rate was 4800 symbols per seconds. Figure 5 shows the position of the two ships during the transmission of this sequence named AIT63 (transmitter: green, receiver: red). The distance and the relative velocity between the transmitter and the receiver were about 640 meters and $v = 2$ m/s, respectively.

To build a burst of symbols, a rate $R_c = 1/2$ convolutional code with constraint length 5 was fed by a block of binary data α_n. An interleaver Π shuffled 22500 coded data $c_{n,i}$. Each set of $m = \log_2(M)$ interleaved coded data $c_{k,i}$ was mapped onto an M-ary complex symbol d_k using a Gray or quasi-Gray mapping. A transmitted burst resulted on the repetition of $m = \log_2(M)$ blocks of $22500/\log_2(M)$ symbols separated by a pilot sequence. As described in Section II, each burst was preceded by a preamble dedicated to frame synchronization and Doppler shift estimation. The burst duration was 25 seconds. The ratio between the information bit rate and the coded bit rate was approximately 0.45.

TABLE I
Main parameters of the sea trials

Modulation type	8-PSK	16-QAM	32-QAM
Coded Bit Rate (bit/s)	14400	19200	24000
Information Bit Rate (bit/s)	6480	8640	10800

In order to highlight the improvements provided by the spatio-temporal equalizer, we analyze the behavior of the receiver in terms of decision-directed minimum mean square error (DD-MSE) at the equalizer output over a duration of 25 seconds. The DD-MSE is estimated in an adaptive manner, by the recursion $DDMSE_{k+1} = \lambda DDMSE_k + (1-\lambda)|z_k - \hat{d}_{k-\Delta}|^2$, where $\lambda = 0.99$ is a forgetting factor.

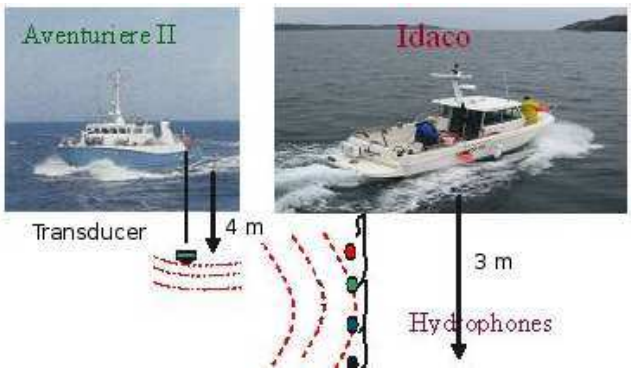

Fig. 4. Sea trial configuration

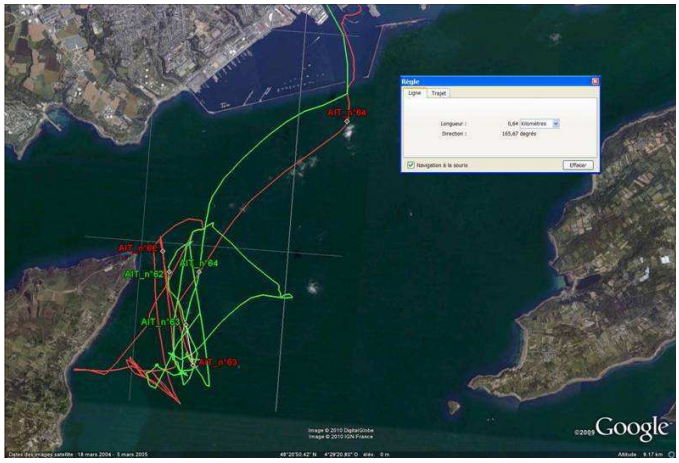

Fig. 5. Brest bay sea trial: record position for the sequence AIT63

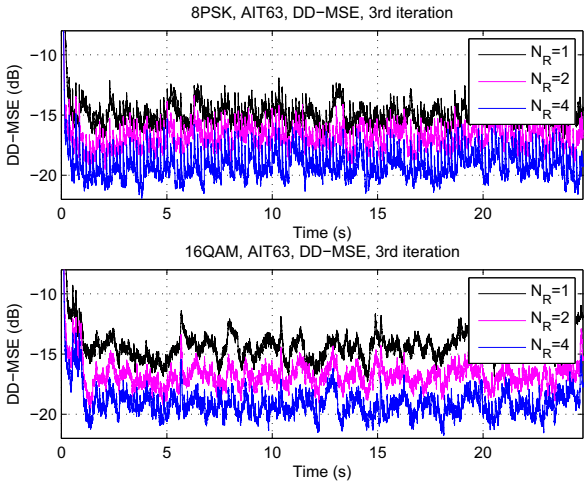

Fig. 6. Sequence AIT63: DD-MSE at the output of the multiple input equalizer versus N_R, 4800 symbols/s, $f_c = 17.5$ kHz

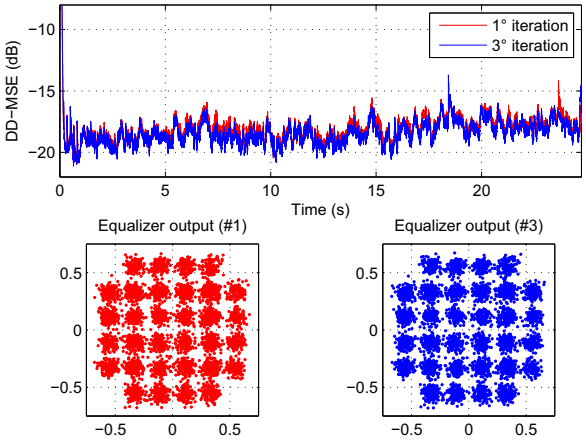

Fig. 7. Sequence AIT63: DD-MSE at the output of the multiple-input equalizer N_R=4, 32QAM, 4800 symbols/s, channel bit rate: 24000 bps, $f_c = 17.5$ kHz, distance=640m, v=2m/s

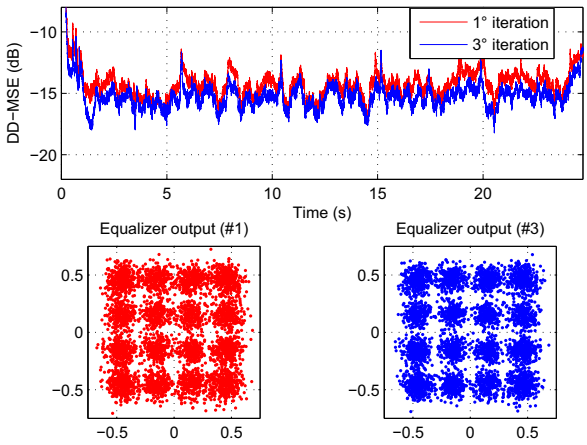

Fig. 8. Sequence AIT63: DD-MSE at the output of a single-input equalizer, $N_R = 1$, 16QAM, 4800 symbols/s, channel bit rate: 19200 bps, $f_c = 17.5$ kHz, distance=640m, v=2m/s

Figure 6 shows the DD-MSE versus the number of hydrophones at the third iteration of the turbo equalizer. A performance gain greater than 6dB is observed when the number of hydropones increases from 1 to 4. This is a well-known result. We recall that the achievable SNR gain offered by the multiple-input equalizer is at least $10\log_{10}(N_R)$ dB when the noise signals at the equalizer inputs are decorrelated.

Figures 7 and 8 give the performance at the first and third iteration of the turbo equalizer for 32-QAM and 16-QAM, respectively. The constellations are plotted for 1 second duration (4800 symbols), from the 10th to the 11th second in the record. For 32-QAM, $N_R = 4$ hydrophones were considered. We first note that for 32-QAM, the performance improvement between the first and the third iteration is rather small. This result can be explained by the fact that the spatio-temporal equalizer drastically reduces ISI at the first iteration, thereby leaving few room for further performance gains in subsequent iterations. For 16-QAM results where $N_R = 1$, we observe a performance improvement in Figure 8 between the first and the third iteration of the turbo equalizer. Note that this gain may be greater than 3dB. We conclude that the turbo equalizer is more attractive for a single-antenna receiver operating in a highly frequency-selective channel, assuming that the SNR is sufficiently high to allow convergence of the iterative process.

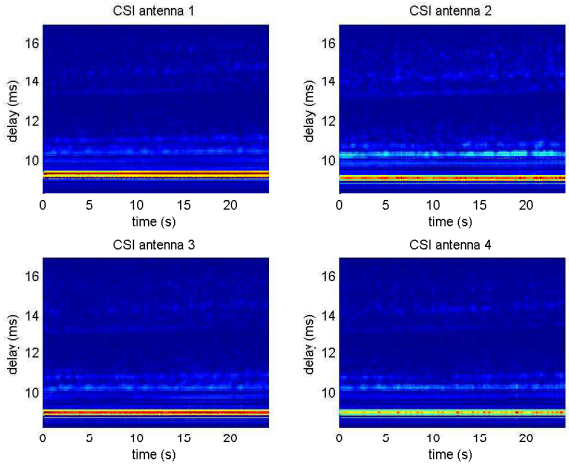

Fig. 9. Sequence AIT63: channel state information, 4800 symbols/s, $f_c = 17.5$ kHz, distance=640m, v=2m/s

TABLE II
SEQUENCE AIT63: BER PERFORMANCE RESULTS

Sequence AIT63, 8-PSK	N_R=1	N_R=2	N_R=4
BER at equalizer output (1st iteration)	2.2e-3	7.2e-4	3.7e-4
BER at decoder output (1st iteration)	0	0	0
BER at equalizer output (3rd iteration)	1.5e-3	6.5e-4	3.7e-4
BER at decoder output (3rd iteration)	0	0	0

TABLE III
SEQUENCE AIT63: BER PERFORMANCE RESULTS

Sequence AIT63, 16-QAM	N_R=1	N_R=2	N_R=4
BER at equalizer output (1st iteration)	1.4e-2	2.3e-3	1.1e-3
BER at decoder output (1st iteration)	2.8e-4	8.9e-6	0
BER at equalizer output (3rd iteration)	6.3e-3	2.0e-3	1.1e-3
BER at decoder output (3rd iteration)	2.4e-4	8.9e-6	0

TABLE IV
SEQUENCE AIT63: BER PERFORMANCE RESULTS

Sequence AIT63, 32-QAM	N_R=1	N_R=2	N_R=4
BER at equalizer output (1st iteration)	0.5	0.5	1.3e-2
BER at decoder output (1st iteration)	0.5	0.5	1.77e-4
BER at equalizer output (3rd iteration)	0.5	0.5	1.0e-2
BER at decoder output (3rd iteration)	0.5	0.5	8.53e-5

The channel state information (CSI) after Doppler shift compensation is shown in Figure 9. The results show that the channel is weakly frequency-selective. These experimental results are in accordance with the well-known fact that the performance improvement offered by the turbo equalizer is all the more important that the channel is highly frequency-selective.

In Tables II, III and IV, we give the bit error rate (BER) at the equalizer output and decoder output versus the iteration and number of hydrophones. The BER was computed over a duration of 25 seconds. The BER at the equalizer output is slightly improved between the first and the third iteration. Note that for 32-QAM with $N_R = 1$ and $N_R = 2$, the experimental SNR was too small, thereby preventing correct synchronization and equalization. This results in a BER of 0.5.

V. Conclusions

Robust single-carrier underwater transmissions based on high-order modulations and adaptive MMSE turbo equalization have been successfully demonstrated in real conditions, with user data rates up to 10 kb/s. Increasing the number of hydrophones was shown to significantly improve the receiver performance. It was also shown that the turbo equalizer is particularly efficient and attractive for underwater transmissions based on a single hydrophone, provided that the SNR is sufficient to allow convergence of the iterative equalization and decoding process. This result may be interesting for industrial considerations where the reduction of the number of hydrophones may lead to costs savings and to a diminution of the equipments size.

References

[1] J. Trubuil, G. Lapierre, and J. Labat, "Real time transmission of images and data through underwater acoustic channel: the trident system," in *Proc. of IGARSS'04*, Anchorage, USA, 2004.

[2] A. Glavieux, C. Laot, and J. Labat, "Turbo equalization over a frequency selective channel," *Proc. of Int. Symp. Turbo Codes*, pp.96-102, Sept. 1997.

[3] M. Tuechler, R. Koetter, and A. Singer, "Turbo equalization: principle and new results," *IEEE Trans. Comm.*, vol. 50,no. 5, pp. 754-767, May 2002.

[4] X. Wang and H. Poor, "Iterative (turbo) soft interference cancellation and decoding for coded CDMA," *IEEE Trans. Commun.*, vol. 47, no. 7, pp.1046-1061, July 1999.

[5] E. Sangfelt, T. Oberg, B. Nilsson, and M. Lundberg Nordenvaad, "Underwater acoustic communication experiments in the baltic sea," in *Proc. of Undersea Defence Technology UDT 2008*, 2008.

[6] J. Choi, R. Drost, A. Singer, and J. Preisig, "Iterative multi-channel equalization and decoding for high frequency underwater acoustic communications," in *Proc. of IEEE Sensor Array and Multichannel signal processing workshop, SAM 2008*, 2008.

[7] C. Polprasert and J. Ritcey, "Performance of the bit-interleaved frequency domain turbo equalization over experimental underwater acoustic channels," in *Proc. of Asilomar conference on signals, Systems and computers*, Pacific grove, CA, 2008.

[8] R. Otnes and T. Eggen, "Underwater acoustic communications: Long-term test of turbo equalization in shallow water," *IEEE Journal of Oceanic engineering*, vol. 33, pp. 321–334, July 2008.

[9] C. Laot and P. Coince, "Experimental results on adaptive mmse turbo equalization in shallow underwater acoustic communication," *Proc. of OCEANS'10*, May 2010.

[10] H. Meyr, M. Moeneclaey, and S. Fechtel, *Digital Communication Receivers: Synchronization, Channel Estimation, and Signal Processing*. New York: Wiley, 1998.

[11] M. Stovanovic, "Guest editorial: Underwater wireless communications," *IEEE Communications Magazine*, vol. 47, p. 78, Jan. 2009.

[12] J. Heidemann, U. Mitra, J. Preisig, M. Stovanovic, and M. Zorzi, "Guest editorial: Underwater wireless communications networks," *IEEE Journal on Selected Areas in communications*, vol. 26, pp. 1617–1616, Dec. 2008.

[13] B. Sharif, J. Neasham, O. Hinton, and A. E. Adams, "A computationaly efficient doppler compensation system for underwater acoustic communications," *IEEE J. Oceanic Eng.*, vol. OE-25, pp. 52–61, Jan. 2000.

[14] L. Freitag, M. Johnson, and D. Frye, "High-rate acoustic communications for ocean observatories-performance testing over a 3000 m vertical path," *Proc. of OCEANS'00*, pp. 1443–1448, Sept. 2000.

[15] J. Tao, Y. Zheng, C. Xiao, T. Yang, and W. Yang, "Equalization and phase correction for single carrier underwater acoustic communications," in *Proc. of OCEANS'08*, Kobe, Japan, April 2008.

[16] C. Berger, S. Zhou, J. Preisig, and P. Willet, "Sparse channel estimation for multicarrier underwater acoustic communication: From subspace methods to compressed sensing," vol. 58, no. 3, pp. 1708-1721, 2010.

[17] Q. Cai, A. Wilzeck, and T. Kaiser, "A compound method for initial frequency acquisition in wcdma systems," in *IEE DSP Enabled Radio Conference*, Southampton, England, 2005.

[18] G. Eynard and C. Laot, "Blind doppler compensation scheme for single carrier digital underwater communications," in *Proc. of OCEANS'08*, Quebec, Canada, 2008.

[19] F. Gardner, *Demodulator Reference Recovery Techniques Suited for Digital Implementation*, ser. ESTEC Contract No. 6847/86/NL/DG. European Space Agency, 1988.

[20] C. Laot, R. Le Bidan, and D. Leroux, "Low complexity linear turbo equalization: A possible solution for EDGE," *IEEE Trans. Wireless. Comm.*, vol. 4, no. 3, pp 965-974, May 2005.

[21] M. Tuechler, A. Singer, and R. Koetter, "Minimum mean squared error equalization using a priori information," *IEEE Trans. Signal processing*, vol. 50, no. 3, pp. 673-683, March 2002.

[22] P. Robertson, E. Villebrun, and P. Hoeher, "A comparison of optimal and sub-optimal map decoding algorithms operating in the log domain," in *Proc IEEE ICC'95*, Seattle, Washington, June 1995.